

Space Intensity Correlations in the Near Field of the Scattered Light: A Direct Measurement of the Density Correlation Function $g(r)$

M. Giglio, M. Carpineti, and A. Vailati

*Dipartimento di Fisica and Istituto Nazionale per la Fisica della Materia, Università di Milano,
via Celoria 16, 20133 Milano, Italy*

(Received 23 December 1999)

We show that the two point intensity correlation in the near field of the scattered light is directly related to the two point density correlation $g(r)$. Preliminary measurements on two sets of calibrated random pinholes of 140 and 300 μm diameters, and on aqueous solutions of latex spheres of 5, 10, and 40 μm are reported. A discussion on the desirability of the technique as a simple and powerful alternative to low angle scattering will be presented.

PACS numbers: 42.30.Ms, 07.60.-j, 42.25.Fx

The intensity of the light scattered from a spatially disordered sample has a speckled appearance, the speckles being generated by the random interference of the scattered elementary spherical waves. While the study of the one point intensity time correlations has proven very useful, and it has generated the technique of intensity fluctuation spectroscopy (IFS) [1], the measurement of the two point (equal time) intensity space correlation function (the size and shape of the speckles) does not provide any useful information. Indeed the Van Cittert and Zernike (VCZ) theorem states that the *far field* space correlation function depends only on the intensity distribution of the scattering volume, and in no way depends on the physical properties of the sample.

In this paper we show that for fluctuations the size of the wavelength of light or larger, the instantaneous spatial intensity correlation function in *near field* scattering yields directly the two point correlation function $g(r)$, a fundamental quantity in statistical mechanics. Alternatively, the Fourier transform of the intensity correlation gives the scattered intensity distribution.

A working formula is derived, and analogies with the IFS are pointed out. We also present data showing the feasibility of the technique. The experimental setup is very unorthodox. It consists of a wide laser beam and of a charge coupled device (CCD) detector positioned so to be flooded with light coming from any scattering direction the system can scatter at. Data are presented for a scattering model (random pinholes) of size 140 and 300 μm and also for solutions of latex spheres of 5, 10, and 40 μm . Advantages with respect to the more conventional low angle scattering technique are discussed.

The Van Cittert and Zernike theorem states that the normalized field correlation function is [2]

$$\begin{aligned} \mu_A(\Delta x, \Delta y) &= \frac{\langle E(x_1, y_1) E^*(x_2, y_2) \rangle}{(\langle E(x_1, y_1)^2 \rangle \langle E(x_2, y_2)^2 \rangle)^{1/2}} \\ &= \frac{\iint I(\xi, \eta) \exp[i \frac{2\pi}{\lambda z} (\xi \Delta x + \eta \Delta y)] d\xi d\eta}{\iint I(\xi, \eta) d\xi d\eta}, \end{aligned} \quad (1)$$

where $\Delta x = (x_1 - x_2)$ and $\Delta y = (y_1 - y_2)$, E is the field in the observation plane $x - y$, λ is the wavelength, and $I(\xi, \eta)$ is the actual intensity distribution of the source in the plane $\xi - \eta$ at a distance z from the observation plane. The theorem holds for sources consisting of point emitters, like atoms. The intensity correlation function $R_I(\Delta x, \Delta y) = \langle I(x_1, y_1) I(x_2, y_2) \rangle$ is then derived by applying the so called Siegert relation [3]:

$$R_I(\Delta x, \Delta y) = \langle I \rangle^2 [1 + |\mu_A(\Delta x, \Delta y)|^2]. \quad (2)$$

Equations (1) and (2) specify that the intensity correlation function is related to the space Fourier transform of the source. In practice, this implies that a source of size D will generate speckles of size $\frac{\lambda}{D} z$ on a screen positioned at a distance z [3].

We start by introducing simple heuristic arguments and crude evaluations for the near field speckles of the scattered light. Let us consider the case of a large diameter beam (diameter D) impinging onto a sample of particles of diameter d larger than the wavelength of light (see Fig. 1a). Most of the power will be scattered in a forward lobe of angular width $\Theta \approx \frac{\lambda}{d}$. Let us consider a small area S (for example, a multielement sensor array) in the immediate vicinity of the scattering volume (see Fig. 1b). Let us assume that we can ignore the transmitted beam (we take care of this problem later on). Although the sample is illuminated over the entire surface of diameter D , the light falling onto the sensing area will come only from a smaller area of diameter D^* . In fact, the brightness of the scattering volume will change as a function of the observation angle in a way that mirrors the scattered intensity distribution. Consequently, for the sensing area, the source region from which light is drawn is a circle with a diameter $D^* = \frac{\lambda}{d} z$, z being the distance of the sensing area from the scattering surface (source regions outside do not contribute appreciably). One can then immediately estimate the size of the speckles $d_{sp} = \frac{\lambda}{D^*} z \approx d$, a remarkable result in many respects. The speckles have the size of the particle diameter, and this value does not depend on the distance z from the sample, provided that $D^* < D$. This has to be compared

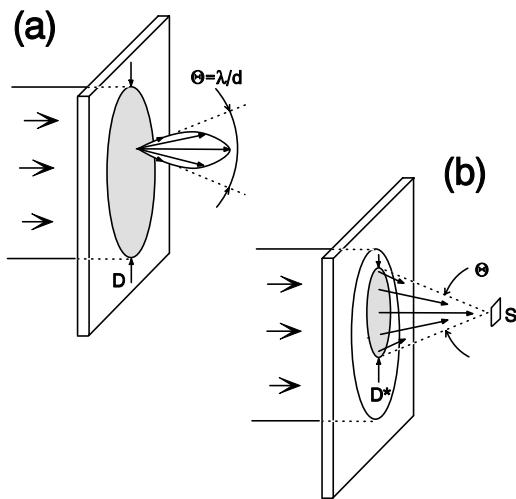


FIG. 1. (a) Low angle scattering. A beam of diameter D impinges onto a sample composed of particles of diameter d . Any zone within D will scatter light into a lobe of angular width $\Theta = \lambda/d$ (the length of arrows indicates scattered intensity). (b) Same sample, as in (a). A sensor S close enough to the sample will draw light only from a zone of radius $D^* < D$. Regions outside, even if illuminated by the main beam, do not feed light to S . Notice that again $\Theta = \lambda/d$.

with far field speckles, whose diameter scales linearly with the distance from the source. Also notice that the actual sample thickness does not matter (provided that the near field condition is met) and that the speckle size does not depend on the light wavelength, an unexpected feature for an interference pattern.

Notice that all the above applies under conditions that are more stringent than the usual “near field” condition [4] for a source of size D , namely, $\frac{\lambda z}{D^2} \ll 1$. In the present case the condition is $D^* \ll D$, which implies $\frac{\lambda z}{Dd} \ll 1$.

To put things in a more quantitative way, we determine the near field intensity correlation by first rewriting the VCZ theorem in a more appropriate form. We notice that Eq. (1) may be rewritten in the following way:

$$\mu_A(\mathbf{r}) \propto \int I(q) e^{i\mathbf{q}\cdot\mathbf{r}} d\mathbf{q}, \quad (3)$$

where $\mathbf{r} = (\Delta x, \Delta y)$, and \mathbf{q} is a vector whose components are $q_x = \frac{2\pi}{\lambda z} \xi$ and $q_y = \frac{2\pi}{\lambda z} \eta$, which coincides with the scattering wave vector for small scattering angles.

Equation (3) is only a different way of writing Eq. (1), and $I(q)$ is the intensity distribution of the source as seen from the observation plane as a function of the scaled “angles” $(2\pi/\lambda)(\xi/z)$ and $(2\pi/\lambda)(\eta/z)$ (we have assumed that the scattering is isotropic). As discussed in the introductory remarks, in the very near field $I(q)$ coincides with the scattered intensity distribution; that is, the Fourier transform of the sample density correlation function $g(r) = \langle \delta n(r) \delta n(0) \rangle / \langle \delta n^2 \rangle$, where δn is the local fluctuation of the particle number density. Then, from Eq. (2), it follows that

$$R_I(r) = \langle I \rangle^2 [1 + |g(r)|^2]. \quad (4)$$

We point out that Eq. (4) closely duplicates the well known relation that holds for the IFS $\langle I(0)I(t) \rangle = \langle I \rangle^2 [1 + |g(t)|^2]$, where $g(t)$ is the time correlation function (see, for example, [5]). It should be noted that for some scatterers the Rayleigh-Gans approximation is invalid (for example, for larger spheres where the Mie theory applies), and, therefore, the pair correlation function $g(r)$ cannot be extracted from the scattered light. It remains true, however, that even in those cases the correlation method permits the determination of the scattered intensity distribution, by calculating the Fourier transform of the experimentally determined intensity correlation [see Eq. (3)].

To determine the spatial intensity correlation of Eq. (4), one must first obtain experimentally the instantaneous intensity distribution of the near field scattered light. In order to evaluate the intensity correlation function with reasonable statistical accuracy it is also imperative to gather intensity distributions over a substantial number of points. To this end a CCD is ideal, the number of pixels being larger than 10^5 . As we shall see, it actually turns out that one frame is enough for a fair acquisition of the correlation function.

We have performed some measurements on a scattering model, opaque metallic screens with pinholes of 140 and 300 μm chemically etched in random positions. The surface fraction occupied by the pinholes is around 10% and 20%, respectively. Experimentally this greatly simplifies the problem, since the scattered field is stationary and also there is no transmitted beam. Being a two dimensional sample, the scattered intensity is simply related to the correlation function of the transparency function $T(x, y)$ with $T = 1$ inside the pinholes and zero outside [6]. A helium neon parallel beam with diameter ($\frac{1}{z^2}$ points) $D = 15$ mm was sent onto the samples, and the speckle field was recorded with a CCD at various distances $z = 50$ cm, $z = 75$ cm, and $z = 100$ cm [7]. The corresponding values for D^* range from 1 to 4.3 mm so that the very near field condition is always met. The rather large dimension of the pinholes was chosen so that the speckles are appreciably larger than the CCD pixel size (typically 9 μm). For each type of pinhole, the measurements performed at the three distances show minute differences. The results are shown in Fig. 2, where the data are compared with the correlation functions of digitized images of the set of pinholes on the metallic screen [8]. The width and shape of the main peak are fairly well reproduced, in spite of the limited number of frames used (four frames on statistically equivalent samples for each type of pinhole).

While the data obtained with the screens prove that near field speckles do mirror the properties of the scatterers, we felt that to assess the desirability of the technique for realistic applications (for example, in colloid physics)

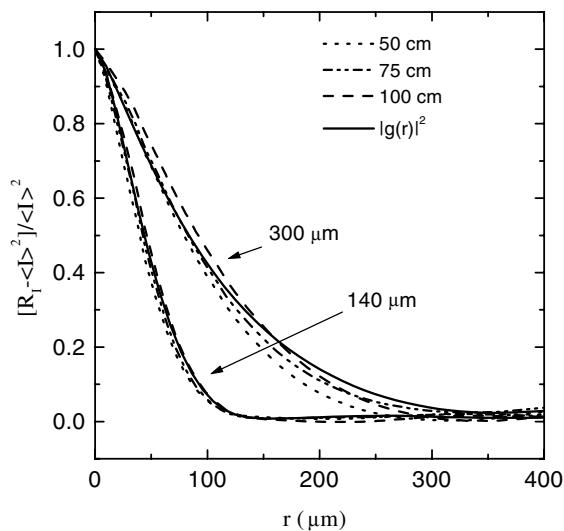


FIG. 2. Measured intensity autocorrelations as a function of displacement r for two sets of randomly positioned pinholes, of 140 and 300 μm in diameter. For both the samples, measurements at three distances are reported, together with $|g(r)|^2$, calculated from the digitized images of the two samples.

measurements had to be taken with particle solutions down in the micron range. In order to do this, three problems had to be solved. The speckles in the near field close to the cell have dimensions around 1 μm and therefore are too small for the available CCD pixel size. Also, one must dispose of the transmitted beam. Finally, the speckle intensity distribution must be frozen at a given instant.

The first two problems have been solved with the simple optical arrangement shown in Fig. 3. A wide parallel beam with diameter ($\frac{1}{e^2}$ points) $D = 12$ mm is sent onto a 1 mm thick sample placed against the large aperture lens L (focal length $f = 80$ mm). A 0.12 mm wire is stretched in the focal plane to intercept the main beam. The CCD is placed a distance z away from the focal plane, with $z \gg f$ (z was made as large as 94 cm). The system demagnifies

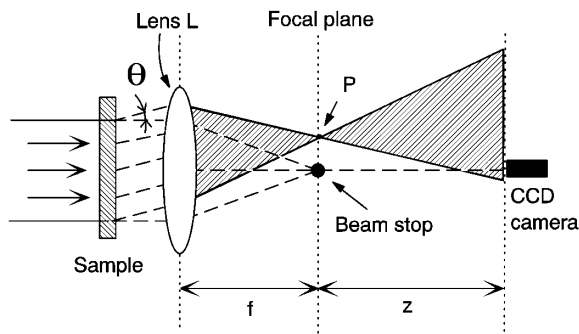


FIG. 3. Optical layout. The main transmitted beam is blocked by a stop in the focal plane. Light scattered at an angle θ (cross hatched in figure) is brought to a focus in P and is in part fed to the CCD. A slight increase in θ would prevent the collection of the scattered light. This maximum angle of acceptance determines the “instrumental” speckle width.

the scattering angles at the lens L by a factor of $M = z/f$, and speckle sizes are increased accordingly. It is illuminating to point out that the technique can be considered as a scaled down version of the classical Hambury-Brown and Twiss [9] experiment where the star intensity distribution is mimicked by the scattered light intensity patch in the focal plane, and the ground based intensity correlations are the CCD intensity correlations. The (unavoidable) presence of the lens and its finite aperture introduces some complication with respect to the lensless arrangement used for the pinholes. A maximum angle of acceptance is introduced, because rays scattered at larger angles, although brought to a focus in the focal plane, may miss the CCD sensor (in Fig. 3 the set of parallel rays scattered at the angle θ is close to the acceptance edge. A slight increase in scattering angle θ would prevent scattered light from reaching the sensor). This necessarily introduces an instrumental response characterized by a function $T(q)$ that describes the gradual decrease and eventually the blocking of the scattered light as the scattering angle is increased. As a consequence there is a minimum, instrumental speckle size. Scattering particles within the instrumental range therefore cast light onto smaller patches in the focal plane, and accordingly the speckles are larger. When the scattered speckles are observed with the CCD in real time, one notices quite vividly that the speckle size changes as the size of the scatterers is changed. Also, for a given sample the speckles “boil” with the same time constant on the whole screen, the time constant getting larger for samples with larger diameter particles. With regard to the third problem mentioned above, these observations also indicate that even with a conventional CCD and a small power He-Ne laser there is no problem in getting instantaneous pattern distributions. Indeed even for the smallest particles that can be studied with the present experimental setup (1 μm diameter) and assuming diffusive motion, the shortest time constant associated to the smallest scattering wave vector yields $\tau_{\min} = 0.125$ sec, a time long compared with the shortest frame exposure available with standard frame grabbers (typically 1/16000 sec). Preliminary results for the speckle intensity autocorrelations for latex particles of 5, 10, and 40 μm are shown in Fig. 4 together with instrumental correlation obtained by using a δ -correlated diffuser [8]. The volume fractions of the solutions are 1.8×10^{-4} , 1.1×10^{-4} , and 1.4×10^{-2} for 5, 10, and 40 μm spheres, respectively. In Fig. 4 we also show the autocorrelation functions calculated from Mie theory as follows. We first calculate $T(q)$ by Fourier transforming the square root of the instrumental correlation. We then calculate the scattered intensity distribution $I(q)$ for the spheres using full Mie theory (at the concentrations used there is no need to account for particle interaction). Finally, we Fourier transform $T(q)I(q)$ and square the result. Fair agreement between the calculated and the experimental autocorrelation functions is found for the 5

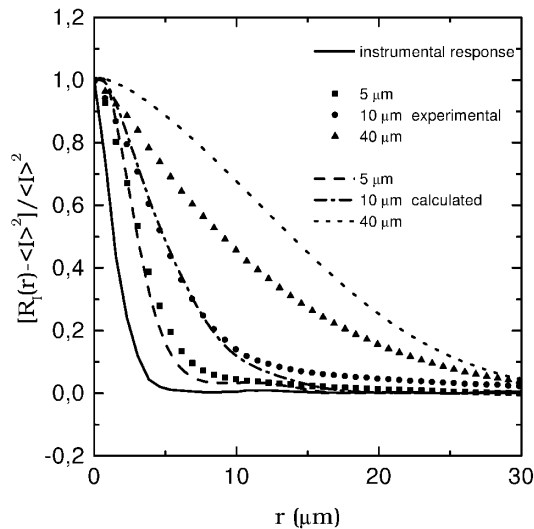


FIG. 4. Measured intensity autocorrelations as a function of the displacement r for water solutions of 5, 10, and 40 μm diameter latex spheres, and for a δ -correlated diffuser (instrumental response). Experimental data are compared with the theoretical autocorrelation functions calculated from Mie theory.

and 10 μm samples, while the results for the 40 μm spheres are in poorer agreement. We think that this is likely due to improper blocking of the very low angle scattering in the focal plane due to the width of the stretched wire, possible poor positioning, and misfocusing. Notice that the three curves are rather smooth and noise free, in spite of the fact that only ten frames per sample have been used.

Let us compare the correlation technique with the more traditional low angle scattering. The essential feature of a scattering layout [10,11] is that the light scattered at a given angle hits the sensors along a circle of given diameter around the optical axis. We believe that the correlation method offers some distinct advantages over the scattering technique. First, there is no need for accurate positioning of the CCD, which can be rather casually placed at a distance z from the focal plane (see Fig. 3). At variance, in low angle scattering one has to know the precise relation between pixels and scattering angles and this is troublesome when the distance z is changed to select a new particle diameter instrumental range. Also, and more important, low angle scattering is plagued by stray light. To mitigate its effects, one has to rely on blank measurements to be subtracted from raw scattering data. The trouble is that stray light is worst at smaller angles, where the sensing elements are necessarily in small number and crowded

close to the optical axis. With the present technique, on the contrary, all the pixels are used in calculating the correlation function for any value of the displacement r and this permits more accurate stray light subtraction.

In conclusion, we stress that the technique in the present form has only one tight requirement, namely, the clean disposal of the transmitted beam that requires accurate focusing and a proper diffraction limited beam stop. It is both conceptually and in practice very simple, and it capitalizes on the high statistical accuracy permitted by the large number of pixels of a CCD and by the good handling capabilities of PCs.

We thank Dr. Fabio Ferri for the gift of the latex samples and for the loan of a Mie scattering algorithm. We also thank Dr. Luca Cipelletti and Dr. Andrea Marchesani for some help with the software. Partial financial support from the Advanced Research Project PRA PROCRY of the Istituto Nazionale per la Fisica della Materia (INFN) is kindly acknowledged.

-
- [1] For an early account on IFS applications, see G.B. Benedek, in the Jubilee Volume in honor of Alfred Kastler, *Polarization, Matter and Radiation* (Presses Universitaires de France, Paris, 1969).
 - [2] See, for example, J.W. Goodman, *Statistical Optics* (Wiley, New York, 1985).
 - [3] See, for example, J.C. Dainty, *Laser Speckle and Related Phenomena* (Springer-Verlag, Berlin, 1975).
 - [4] See, for example, A. Yariv, *Quantum Electronics* (Wiley, New York, 1967).
 - [5] B. Berne and R. Pecora, *Dynamic Light Scattering* (Wiley, New York, 1974).
 - [6] J.W. Goodman, *Introduction to Fourier Optics* (McGraw-Hill Book Company, New York, 1968).
 - [7] For very large objects the near field is not really near, since one must let the diffraction figures from various objects interfere. This leads to the additional condition $D^* = \frac{\lambda}{d}z \gg \delta$, where δ is the typical distance between scatterers.
 - [8] Experimental correlation functions shown in Figs. 2 and 4 are calculated according to the following procedure. We first calculate the fast Fourier transform of the intensity distribution. We then square the result. The autocorrelation is then obtained by antitransforming the power spectrum.
 - [9] R. Hambury-Brown and R. Q. Twiss, *Nature (London)* **178**, 1046 (1956).
 - [10] M. Carpineti, F. Ferri, M. Giglio, E. Paganini, and U. Perini, *Phys. Rev. A* **42**, 7347 (1990).
 - [11] F. Ferri, *Rev. Sci. Instrum.* **68**, 2265 (1997).